

A Stand-Alone Wind Energy Conversion System with FLC Based Proficient UPF Rectifier

L. Baya Reddy*, B. Murali Mohan**, P. Vidya Prasanna***

Abstract: In this paper, a close solidarity force variable front-end rectifier utilizing two present control routines, specifically, normal current control and hysteresis current control, is considered. This rectifier is interfaced with a settled pitch wind turbine driving a changeless magnet synchronous generator. A conventional diode-span rectifier with no present control is utilized to contrast the execution and the proposed converter. Two steady wind velocity conditions and a changing wind rate profile are utilized to ponder the execution of this converter for an evaluated stand-alone load. The parameters under study are the info force component and aggregate symphonious mutilation of the data streams to the converter.

1. INTRODUCTION

The Solar, wind, and tides are a portion of the option wellsprings of vitality that are utilized to create energy to beat the constraints of routine fossil fills, for example, coal, normal gas, and oil. They are ecologically well disposed and offer boundless potential for usage as they are accessible in wealth for nothing. The era of electric vitality from wind frameworks has become rapidly from a worldwide introduced force of 4.8 GW in 1995 to 58 GW in 2005, at a normal yearly development rate of 24%. Starting 2011, it is assessed that 83 nations around the globe utilization wind power on a business premise. Wind vitality frameworks can be utilized as either remain solitary frameworks or network associated frameworks. Power generation closer to the heap focuses adds to lessened expenses and expanded vitality request fulfilment. Since most of the writing identified with little scale wind turbine frameworks manages network associated frameworks and the investigation exhibited can't be reached out to remain solitary frameworks, there is a requirement for investigation of wind vitality as a vital force hotspot for secluded destinations, i.e., remain solitary wind frameworks.

The centre of this work is on the front-end converter configuration for a stand-alone wind vitality change framework (WECS). The point of the outlined converter is to encourage high-power component operation and accomplish adequate symphonious substance of data streams at the generator stator terminals and to separate the greatest conceivable genuine force at the changeless magnet synchronous generator (PMSG)–power-electronic-converter interface.

This has been accomplished by utilizing two present control systems, the normal current control (ACC) and hysteresis current control (HCC), for the front-end rectifier. This rectifier is a three-stage converter utilizing three static bidirectional changes to perform line current forming and guaranteeing high-information force component operation. Protected entryway bipolar transistors (IGBTs) are utilized as a part of the development of these switches on the grounds that the force necessity is just a little portion of the rectifier's amid the converter operation.

* Assistant Professor Dept. Of EEE/A.I.T.S Email: reddy.baya@gmail.com

** Assistant Professor Dept. Of EEE/A.I.T.S Email: muralimohanaits1@gmail.com

*** PG Scholar Dept. Of EEE/A.I.T.S Email: prasannav230@gmail.com

This keeps the weights on the switches low and empowers the utilization of low-power gadgets, prompting a noteworthy lessening in cost.

2. STAND-ALONE WECS

Wind is a profoundly stochastic vitality source. There is likewise an in number reliance between the streamlined attributes of the wind turbine, the generator's rotor rate, and the measure of force that can be extricated from the wind. Thus, it gets to be important to actualize a control strategy that will empower the extraction of the most extreme force from the framework under all conceivable working conditions. The accompanying areas highlight the real parts of a stand-alone WECS.

2.1. Wind Turbine

Wind turbines are grouped taking into account the quantity of edges and the pivot about which they are mounted. Ordinarily, the three sharp edge level pivot wind turbine is favoured because of better execution and additionally the even dispersion of varieties in wind speed from the rotors to the drive shaft. It is likewise equipped for accomplishing better power coefficient.

The yield mechanical force of the wind turbine is given by the 3D square law mathematical statement

$$P_m = 0.5 \rho c_p A U_w^3 \text{ (Watts)} \quad (1)$$

Where, ρ is the thickness of air (in $\text{kg} \cdot \text{m}^3$), C_p is the force coefficient, A_n is the region cleared by the wind turbine rotor (in square meter), U_w is the wind speed (in meters every second). The force coefficient is a component of the tip speed proportion λ and the sharp edge pitch edge β . It depicts the effectiveness of the wind turbine in changing over the vitality present in wind into mechanical force. The tip speed proportion λ may be characterized as the proportion of the rate at which the external tip of the turbine edge is moving to the wind speed. It is given by the mathematical statement

$$\lambda = (r\omega_m)/U_w \quad (2)$$

The sharp edge pitch point \hat{a} is characterized as the edge at which the wind contacts the edge surface. The expression for force coefficient is given as

$$c_p(\lambda, \beta) = c_1 \left(\left(\frac{c_2}{\lambda_i} \right) - c_3 \beta - c_4 \right) e^{\left(\frac{-c}{\lambda_i} \right)} + c_{6,\lambda} \quad (3)$$

Here, the coefficients $C1 = 0.5176$, $C2 = 116$, $C3 = 0.4$, $C4 = 5$, $C5 = 21$, and $C6 = 0.0068$, and

$$(1/\lambda_i) = 1(\lambda + 0.08\beta) - 0.035/(\beta^3 + 1) \quad (4)$$

It is legitimate to accept pitch edge to be zero for low to medium wind speeds. Henceforth, in this work, $\beta = 0^\circ$. To accomplish most extreme extraction of force from the framework, the tip speed proportion and force coefficient must be kept up near the ideal qualities and differed by varieties in the wind rate conditions. The mechanical torque of the framework is given by the mathematical statement

$$T_m = P_m / \omega_m \quad (\text{N} \cdot \text{m}). \quad (5)$$

2.2. Choice of WTG

There are numerous generator sorts which discover application in a WECS, for example, squirrel-confine prompting generator, doubly bolstered incitement generator (DFIG), and the PMSG. Of these, the last two are most prevalently utilized as a part of WECS. In this paper, a PMSG is utilized as the wind turbine generator (WTG) in light of its

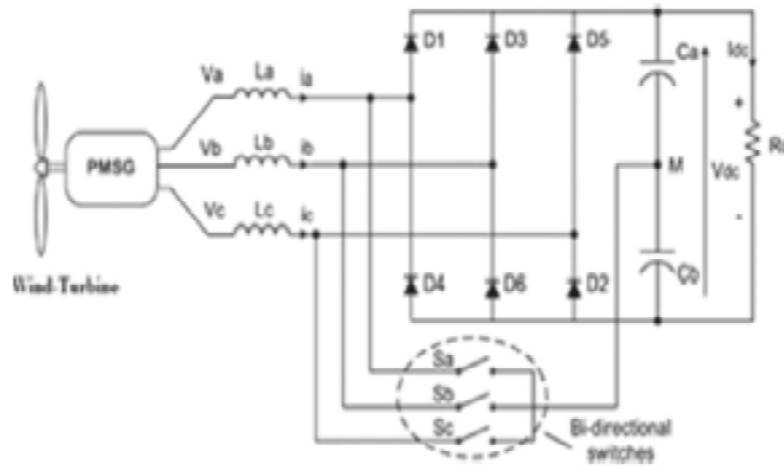


Figure 1: Front-end UPF rectifier.

minimal size, higher force thickness, decreased misfortunes, high unwavering quality, and power. The most noteworthy favourable position is the disposal of the gearbox, in examination to the DFIG. Hence, the wind turbine can be straightforwardly coupled to the generator. Such frameworks are called direct commute frameworks and are most suitable for low-speed working.

Attributable to the ringer moulded nature of wind turbine force bends, the WTG is worked in the variable rate mode keeping in mind the end goal to accomplish most extreme force from the occurrence wind. The parameters of the wind turbine and the direct determined PMSG utilized are given in the Appendix.

2.3. Front-End Power Converter

In most existing little scale wind turbine frameworks, the favoured decision for a front-end converter is a diode-span rectifier on account of its innate straightforwardness. In any case, because of their nonlinear nature, diode-span rectifiers infuse symphonious parts into the framework, prompting an expanded aggregate consonant twisting (THD) of data current, which is communicated as expanded misfortunes because of warming, breakdown of gear, and diminished general effectiveness of the framework.

Alongside info current THD, the PMSG working force element is another parameter of hobby. In the event that the PMSG works at a slacking force element, it prompts creation of receptive force at the stator terminals, in this manner diminishing the greatest usable (genuine) power that the generator is fit for delivering. Consequently, it is alluring that the front-end converter is fit for keeping up high power component and great quality streams, i.e., demonstrate great current control capacity.

2.4. ACC Method

The normal current controller utilizes the slope examination strategy. The prompt current blunder is computed and encouraged to a proportional–integral (PI) controller, as demonstrated in Fig. 3. The yield of the PI controller is sustained to a comparator alongside a saw-tooth bearer. On the off chance that convergences are gotten, the slip is compelled to stay inside of the band determined by the bearer waveform which is regular to all the three stages. The necessary term diminishes the relentless state mistake between the reference and genuine streams.

According to Fig. 1, the accompanying comparisons have been acquired:

$$\begin{aligned}
 L(di_a/dt) &= v_a - (v_{AM} + v_{MO}) \\
 L(di_b/dt) &= v_b - (v_{BM} + v_{MO}) \\
 L(di_c/dt) &= v_c - (v_{CM} + v_{MO})
 \end{aligned} \tag{6}$$

Where, i_a , i_b , and i_c are the inductor streams; v_a , v_b , and v_c are the source voltages from the PMSG; v_{MO} is the voltage of mode M in reference to the unbiased point N; v_{AM} , v_{BM} , and v_{CM} are the voltages at hubs A, B, and C alluding to hub M. These voltages can be communicated as takes after, where $sign(i_a)$, $sign(i_b)$, and $sign(i_c)$ rely on upon the extremity of inductor stream.

$$\begin{cases} v_{AM} = sign(i_a)(1-s_a)\left(\frac{Vdc}{2}\right) \\ v_{BM} = sign(i_b)(1-s_b)\left(\frac{Vdc}{2}\right) \\ v_{CM} = sign(i_c)(1-s_c)\left(\frac{Vdc}{2}\right) \end{cases} \tag{7}$$

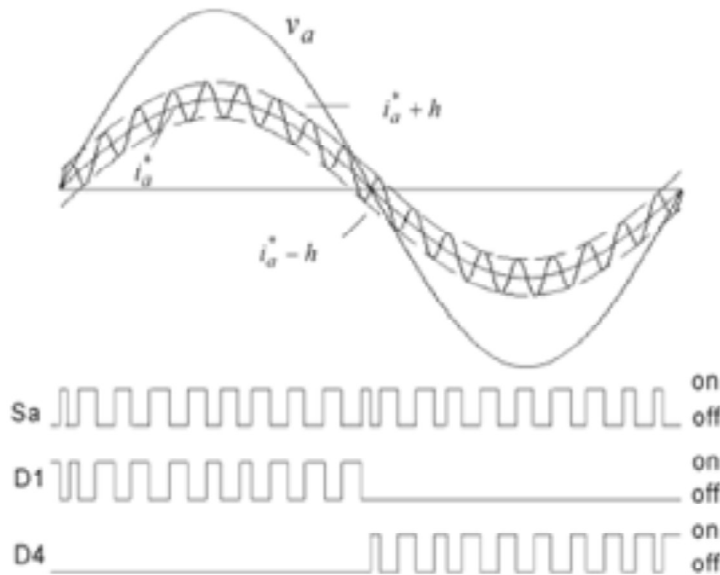


Figure 2: Switching operation for phase “a”: Sa is the bidirectional switch for phase “a,” and D1 and D4 are the upper and lower bridge diodes, respectively

Case in point,

$$Sign(i_a) = \begin{cases} 1, & \text{if } i_a \geq 0 \\ -1, & \text{if } i_a < 0 \end{cases} \tag{8}$$

Here, s_a , s_b , and s_c are the exchanging states for the three bidirectional switches S_a , S_b , and S_c . “1” is for switch-on, and “0” is for switch-off. An external dc voltage controller has been actualized to keep up the dc-join voltage equalization over the capacitors. Nonetheless, there is a condition which expresses that, when a large portion of the dc-join voltage is lesser than the stage voltage, the powerful component condition is not accomplished.

2.5. HCC Method

In this present control technique, the bidirectional switches are controlled in light of the stage current lapse falling inside of the hysteresis band. The decision of the hysteresis band is discriminating in deciding the exchanging states and the forming of the rectifier streams. Fig. 4 demonstrates the exchanging operation for stage “an” of the UPF

converter utilizing HCC. The exchanging signs for the bidirectional switches are as per the following, where h is the hysteresis band.

3. CONVERTER TOPOLOGY

A customary wind framework ordinarily utilizes an uncontrolled diode-span rectifier–inverter framework. It demonstrates an incomprehensible debasement in execution under shifting wind conditions. The line current at the information of the conventional rectifier shows high consonant contortion, adding to expanded misfortunes and poor influence element at the PMSG–rectifier interface. This infers that the force removed by the conventional ac–dc–ac converter is lower than the appraised force of the wind-turbine–PMSG framework. This highlights the significance of a present control technique to guarantee great force extraction, enhanced nature of current and voltage waveforms, and high productivity. Therefore, in this work, the diode rectifier is supplanted with a front-end converter utilizing current control systems for productive genuine force extraction.

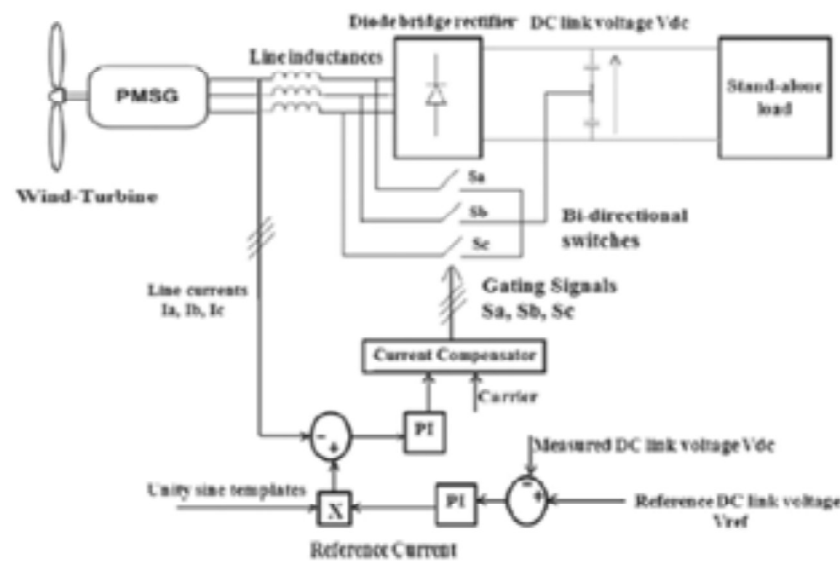


Figure 3: Schematic of the UPF converter in the wind generator system employing the ACC method.

The schematic of the wind-turbine-driven PMSG interfaced with the close UPF converter utilizing the ACC strategy is demonstrated in Fig. 5. Three bidirectional switches are associated between the data of the converter and the basic point at the dc transport join at the yield of the converter nourishing a standalone load. In this paper, the stand-alone load is displayed as a sinusoidal heartbeat width-tweak (PWM) inverter joined with a star-associated three-stage burden, portrayed in the Appendix.

The wind turbine is displayed by. The information and yield of the wind turbine square are the wind speed and the mechanical torque T_m , separately. Mechanical torque T_m is the information to the PMSG square. I_a , I_b , and I_c are the generator streams which are the data line ebbs and flows to the front-end rectifier. In the ACC system, the solidarity sine current layouts are created, which are contrasted with the genuine line streams with get the blunder. This prompt blunder is encouraged to the PI controller whose parameters should be picked painstakingly. The incline examination strategy is performed to produce the gating signs S_a , S_b , and S_c for the switches. The schematic utilized for the HCC is indicated in Fig. 6, where the solidarity sine references are then sent to the hysteresis current controller alongside the real stage streams to create exchanging signs for the three switches. The routine HCC system is taking into account the arbitrary recurrence technique for control and is attractive in numerous applications because of favourable circumstances, for example, simple execution, great exactness, and high heartiness. The main disadvantage is the arbitrary exchanging recurrence, which is lesser than the recurrence received for the ACC.

SIMULATION RESULTS

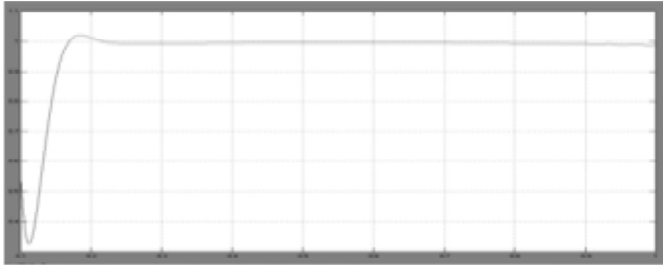
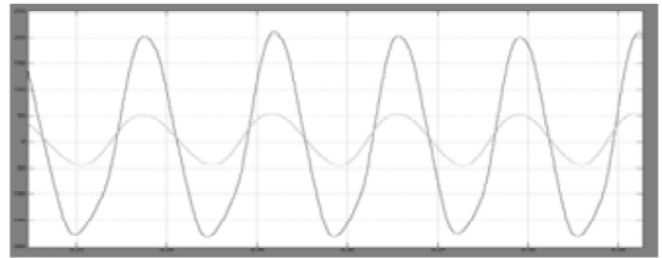
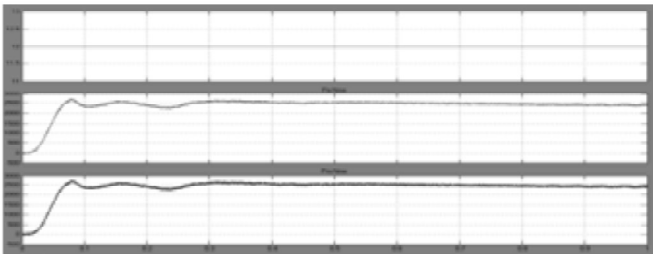


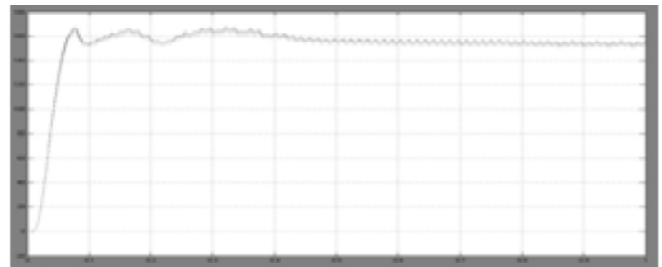
Figure 4: Performance parameters of the UPF rectifier using ACC at a rated wind speed of 12 m/s. (a) Input power factor of the front-end rectifier employing ACC at a rated wind speed of 12 m/s.



(b) FFT of phase "a" current and voltage to frontend rectifier employing ACC at a rated wind speed of 12 m/s.



(c) Mechanical, PMSG, and dc output powers of the system employing ACC at a rated wind of speed 12 m/s.



(d) DC bus capacitor voltages of the system employing ACC at a rated wind speed of 12 m/s.

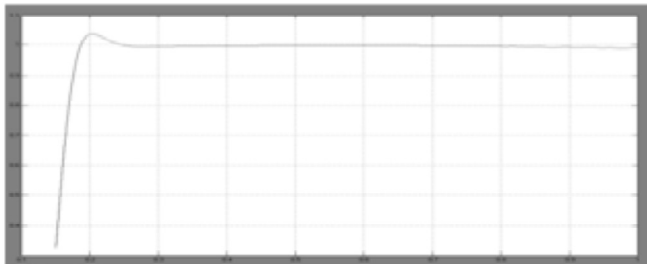
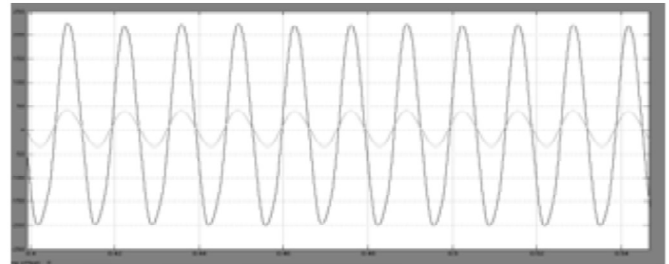
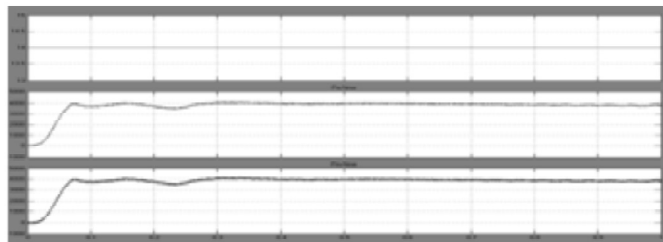


Figure 5: Performance parameters of the UPF rectifier employing ACC at a wind speed of 14 m/s. (a) Input power factor of the front-end rectifier employing ACC at a wind speed of 14 m/s.



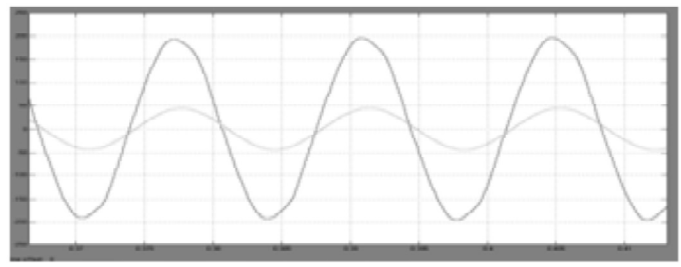
(b) FFT of phase "a" current to front-end rectifier employing ACC at a wind speed of 14 m/s.



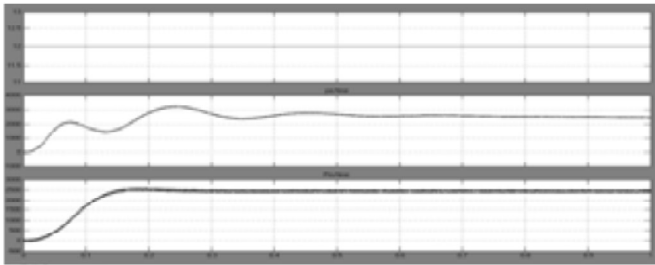
(c) Mechanical, PMSG, and dc output powers of the system employing ACC at a wind speed of 14 m/s.



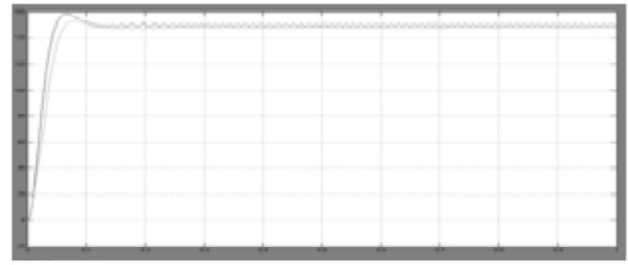
Figure 6: Performance parameters of the UPF rectifier using HCC at a rated wind speed of 12 m/s. (a) Input power factor of the front-end rectifier employing HCC at a rated wind speed of 12 m/s.



(b) FFT of phase "a" current and voltage to frontend rectifier for HCC at a rated wind speed of 12 m/s.



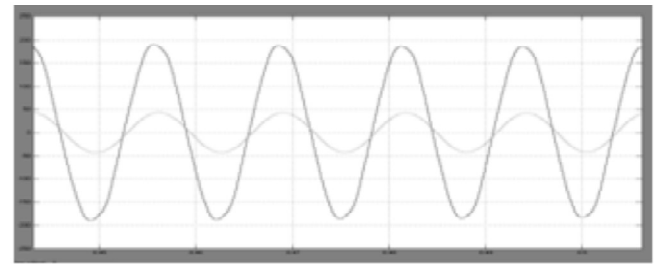
(c) Mechanical, PMSG, and dc output powers of the system for HCC at a rated wind speed of 12 m/s.



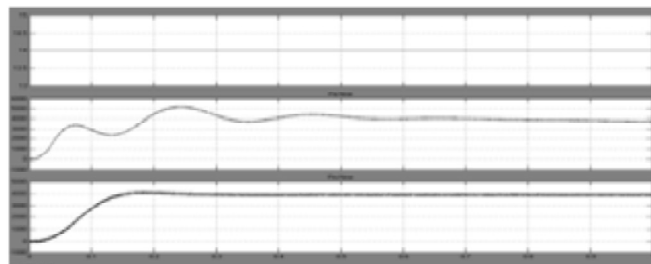
(d) DC bus capacitor voltages for HCC at a rated wind speed of 12 m/s.



Figure 7: Performance parameters of the UPF rectifier using HCC at a wind speed of 14 m/s. (a) Input power factor of the front-end rectifier employing HCC at a higher wind speed of 14 m/s.



(b) FFT of phase "a" current and voltage to frontend rectifier for HCC at a higher wind speed of 14 m/s.



(c) Mechanical, PMSG, and dc output powers of the system for HCC at a higher wind speed of 14 m/s.

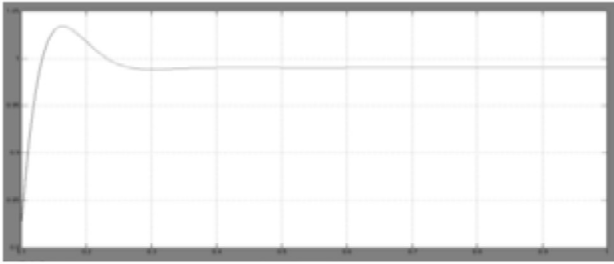
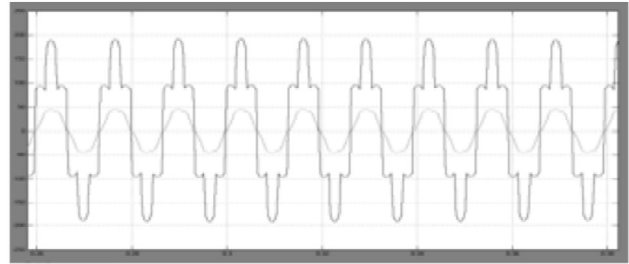
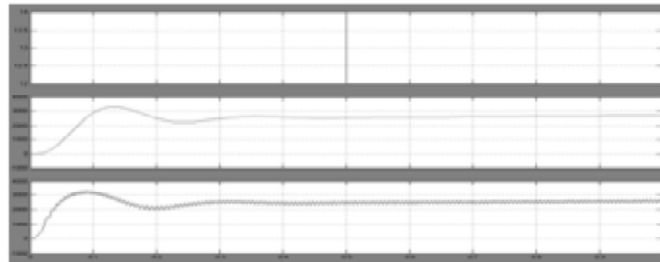


Figure 8: Performance parameters of the diode-bridge rectifier at a rated wind speed of 12 m/s. (a) Input power factor of the front-end diode-bridge rectifier at a rated wind speed of 12 m/s.



(b) FFT of phase "a" current and voltage of front-end diode-bridge rectifier at a rated wind speed of 12 m/s.



(c) Mechanical, PMSG, and dc output powers of the system for front-end diode-bridge rectifier at a rated wind speed of 12 m/s.

The extension of the given proposed system can be done by adding Fuzzy logic controller in The place of PI controller.

4. FUZZY LOGIC CONTROL

Fuzzy method of reasoning ends up being better known as a result of overseeing issues that have insecurity, vagary, parameter mixture and especially where system model is complex or not exactly described in experimental terms for the created control movement. The beginning of the fuzzy reason introduced by Zadeh is a blend of feathery set speculation and fuzzy inference system (FIS). Parts of a fluffy set have a spot with it with a certain degree, called level of support. The level of enlistment is a result of mapping the data to particular models using a membership function (MF). The development which maps the predetermined information to the output using fluffy basis is known as fuzzy derivation. A fuzzy derivation system can be named:

- (a) Fuzzification: this is the methodology of changing over any new regard to for all intents and purposes identical to etymological variable in perspective of certain MF,
- (b) Inference motor: reproduces human decision,
- (c) Learning base: includes MF definitions and crucial rules like IF-THEN or it is blend of condition part with their related standards
- (d) Defuzzification: is the development of changing the fuzzy output into a crisp numerical quality. In this undertaking rule control information variable is the DC-link voltage error and output of FLC is the crest estimation of the reference source current.

EXTENSION RESULTS

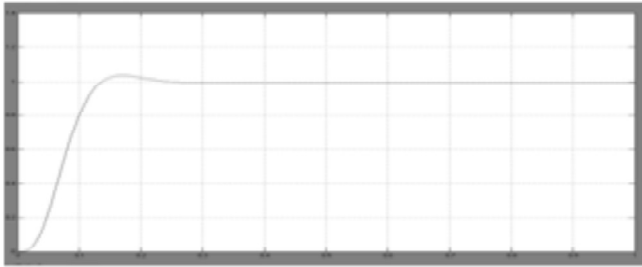
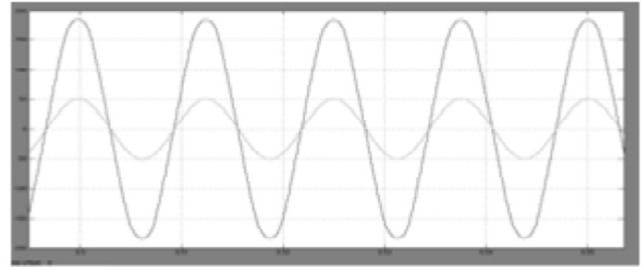
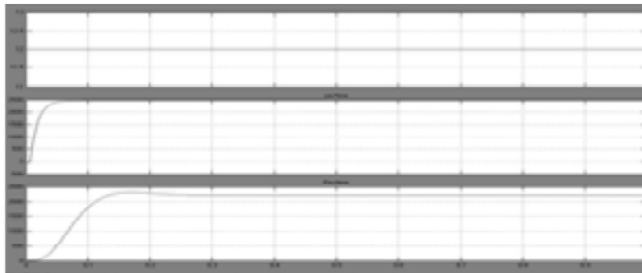


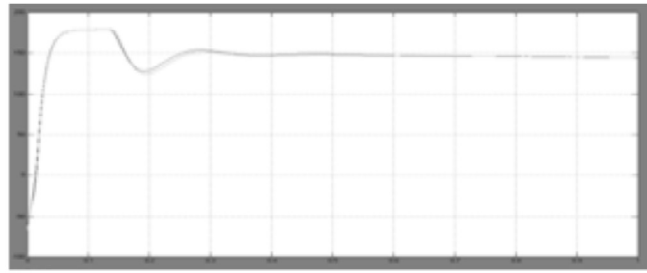
Fig. 9. Performance parameters of the UPF rectifier using HCC at a rated wind speed of 12 m/s. (a) Input power factor of the front-end rectifier employing HCC at a rated wind speed of 12 m/s.



(b) FFT of phase "a" current and voltage to front-end rectifier for HCC at a rated wind speed of 12 m/s.



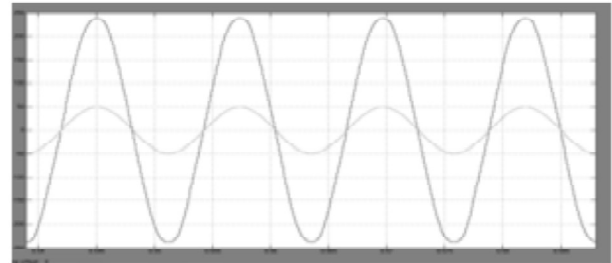
(c) Mechanical, PMSG, and dc output powers of the system for HCC at a rated wind speed of 12 m/s.



(d) DC bus capacitor voltages for HCC at a rated wind speed of 12 m/s.



Fig. 10. Performance parameters of the UPF rectifier using HCC at a wind speed of 14 m/s. (a) Input power factor of the front-end rectifier employing HCC at a higher wind speed of 14 m/s.



(b) FFT of phase "a" current and voltage to front-end rectifier for HCC at a higher wind speed of 14 m/s.



(c) Mechanical, PMSG, and dc output powers of the system for HCC at a higher wind speed of 14 m/s.

5. CONCLUSION

In this paper, a WECS interfaced with an UPF converter nourishing a stand-alone load has been examined. The utilization of basic bidirectional switches in the three-stage converter results in close UPF operation. Two present control systems, i.e., ACC and HCC, have been utilized to perform dynamic info line current forming, and their exhibitions have been looked at for changed wind rate conditions. The nature of the line streams at the data of the converter is great, and the consonant bends are inside of as far as possible as indicated by the IEEE 519 standard for a stand-alone framework. A powerful element is accomplished at the information of the converter, and the voltage kept up at the dc transport connection shows astounding voltage parity. The proposed technique yields better execution contrasted with a customary uncontrolled diode span rectifier framework commonly utilized in wind frameworks as the front-end converter. At long last, a research centre model of the UPF converter driving a stand-alone load has been created, and the ACC and HCC momentum control systems have been tried for correlation. The HCC current control procedure was observed to be predominant and has better voltage adjusting capacity. It can therefore be a brilliant front-end converter in a WECS for stand-alone loads or lattice association.

References

- [1] C. E. A. Silva, D. S. Oliveira, L. H. S. C. Barreto, and R. P. T. Bascope, "A novel three-phase rectifier with high power factor for wind energy conversion systems," in Proc. COBEP, Bonito-Mato Grosso do Sul, Brazil, 2009, pp. 985–992.
- [2] Online.Avaliable:http://en.wikipedia.org/wiki/Wind_energy
- [3] M. Druga, C. Nichita, G. Barakat, B. Dakyo, and E. Ceanga, "A peak power tracking wind system operating with a controlled load structure for stand-alone applications," in Proc. 13th EPE, 2009, p. 19.
- [4] S. Kim, P. Enjeti, D. Rendusara, and I. J. Pitel, "A new method to improve THD and reduce harmonics generated by a three phase diode rectifier type utility interface," in Conf. Rec. IEEE IAS Annu. Meeting, 1994, vol. 2, pp. 1071–1077.
- [5] A. I. Maswood and L. Fangrui, "A novel unity power factor input stage for AC drive application," IEEE Trans. Power Electron., vol. 20, no. 4, pp. 839–846, Jul. 2005

This document was created with Win2PDF available at <http://www.win2pdf.com>.
The unregistered version of Win2PDF is for evaluation or non-commercial use only.
This page will not be added after purchasing Win2PDF.